Thermochimica Acta, 188 (1991) 95–117
Elsevier Science Publishers B.V., Amsterdam

Quantitative description of isothermal and non-isothermal nanocrystalline crystallization of $Co_{33}Zr_{67}$

I.R. Göbel [a] and M.M. Nicolaus [b]

[a] *Institut für Allgemeine Mechanik und Festigkeitslehre, Technische Universität Braunschweig, D-3300 Braunschweig (Germany)*
[b] *Institut für Werkstoffe, Technische Universität Braunschweig, D-3300 Braunschweig (Germany)*

(Received 2 January 1991)

Abstract

The alloy $Co_{33}Zr_{67}$ crystallizing from the amorphous state was examined calorimetrically. The theory used for the description of the energy release is based on a Markov process that allows the description of static and dynamic (re-)crystallization. The Markov model is used in a simplified form as a differential equation, together with a transition probability derived from the classical theory of Johnson, Mehl, Avrami and Kolmogorov. The Avrami parameters are determined from isothermal experiments. It is shown that the slopes in the Avrami plot should be determined for low degrees of crystallization in order to obtain good agreement between theory and experiment. Additionally, the crystallization process is characterized by a temperature-dependent incubation time that has to be included in the model. It is finally shown that non-isothermal processes can be calculated with sufficient accuracy from the isothermal results, demonstrating that the Markov model gives a physically meaningful description of crystallization.

INTRODUCTION

The metallic glass $Co_{33}Zr_{67}$ crystallizes at temperatures above about 669 K (396 °C) into a nanocrystalline structure. The isothermal and non-isothermal crystallization process, the latter at a constant heating rate, was observed calorimetrically, giving as experimental output

$$\dot{E}(t) = \dot{x}(t) E_{\text{stor}} \tag{1}$$

where $\dot{E}$ is the rate of energy release, t is the time, $\dot{x}$ is the time derivative of the degree of crystallization, x, and E_{stor} is the stored energy that is released on crystallization. From eqn. (1), the degree of crystallization is derived

$$x(t) = E(t)/E_{\text{stor}} \tag{2}$$

The degree of crystallization characterizes the transformation process. The discussion of experimental results is in general done with the theory of

0040-6031/91/$03.50

Johnson, Mehl, Avrami and Kolmogorov (JMAK) [1], which determines x from

$$x(t) = 1 - \exp(-\alpha t^n) \tag{3}$$

where α and n are empirical parameters that have to be adapted to the experimental data. In an Avrami plot, $\log|-\ln|1-x||$ versus $\log|t|$, n is ideally the slope of a linear curve when isothermal data are used. The transformation of eqn. (3) from isothermal to non-isothermal processes is still under discussion (for example by Schmidt [2]). Very often, systematic deviations from the JMAK theory occur in the last half or third of the process, where the real process is in most cases slower than predicted by the JMAK theory (see for example Schönborn and Haessner [3]).

In this paper, a model for recrystallization and crystallization based on a Markov process (Göbel [4]) is used for the quantitative description of the crystallization processes observed on $Co_{33}Zr_{67}$. The Markov model is reduced to a single differential equation and provided with a transition probability (TP) that behaves according to the theory of JMAK. Thus, both models and their results can be compared. Pursuing the concept of the Markov model, a strategy is developed for parameter fitting that is different from the classical proceedings based on the Avrami plot, but gives nonetheless very convincing and good results. For $Co_{33}Zr_{67}$, the experimental curves in the Avrami plot are highly non-linear (Fig. 1(a)) so that the determination of a single slope is a problem. Moreover, not only is the parameter α in eqn. (3) temperature dependent, but so also is n. The crystallization process has an incubation time which distorts the curves in the Avrami plot (cf. Fig. 1(a)

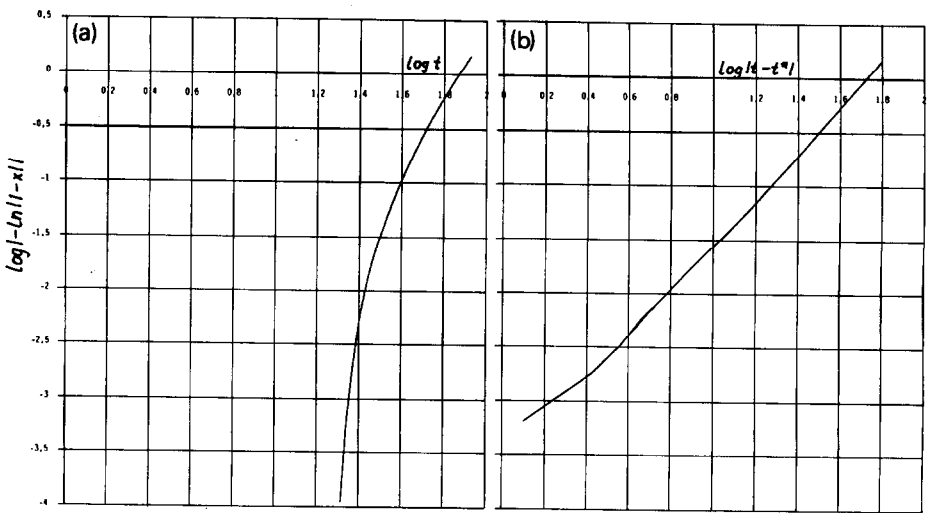

Fig. 1. Avrami plots for the experimental data at $T = 669$ K: (a) classical Avrami plot; (b) time-transformed Avrami plot with the incubation time t^*.

with Fig. 1(b)). Finally, there are deviations between experimental results and the JMAK theory for the last 30% of the process (cf. Fig. 6(c)), which can be taken account of by the Markov model by introducing an additional transition probability for processes not included in the JMAK theory. After having determined the parameters of the crystallization process from isothermal experiments, non-isothermal experiments can be predicted very well by the Markov model. The most striking feature of the process is that it does not depend on the temperature gradient, but only on the actual temperature. A Markov process, as it has no memory, cannot react on time-dependent gradients, and thus it is an adequate mathematical model for a crystallization process.

In the present paper, firstly the experiments are described. In the following section, the Markov model is introduced and compared with the JMAK theory. The next section deals with the determination of the Avrami parameters α and n of eqn. (3), the incubation time, and the transition probability that corrects the JMAK behaviour. The classical methods of parameter determination for the JMAK theory are compared with the methods developed here using the Markov model. In the last section, the results of non-isothermal calculations are compared with experimental results.

EXPERIMENTAL

Calorimetric measurements were used to study the crystallization reaction of the metallic glass $Co_{33}Zr_{67}$. Amorphous ribbons of the material were prepared by melt spinning in vacuum (carried out at the "Kristallabor der physikalischen Institute" at the University of Göttingen) and studied by X-ray diffraction and transmission electron microscopy investigations. After cleaning the $Co_{33}Zr_{67}$ ribbons in an ultrasonic bath with methanol, they were sealed into aluminium pans or Duran glass containers under vacuum in order to prevent oxidation of the sample surfaces. During the calorimeter run the measurement cells were flushed with an inert gas.

The course of crystallization was followed by two different types of calorimeter, a differential scanning calorimeter (Perkin–Elmer DSC7) and a differential heatflux calorimeter (MCB Thermalanalyse, Grenoble). The first was used in the isothermal mode and the second only in the isochronal mode.

Both measuring systems allow digital data registration and therefore evaluation with personal computer. The measured signals were always corrected using a de-smearing algorithm [5].

THE MARKOV MODEL

The basic model is a Markov process

$$z_{t+\delta t} = \boldsymbol{M} z_t \tag{4}$$

where z_t is the distribution of flow units at time step t, and $\boldsymbol{M}$ is the stochastic matrix. The Markov model is explained in detail by Göbel [4] or, without recrystallization, by Steck [6]. It describes the movement of flow units along a scale of internal stresses by TPs of hardening, recovery and recrystallization. The site of the flow units on the scale of internal stresses characterizes the actual state of the material. The TPs of hardening and recovery can move flow units one step on the scale of internal stress in the forward and backward directions, whereas the TP of hardening moves flow units in the forward direction and the TP of recovery moves them backwards. The TPs of recrystallization bring back the flow units into the region of the internal stress scale where they started out initially, thus describing the transformation of a distorted into an undistorted material, as is the case in recrystallization.

If only one class of internal stress is considered to characterize the undistorted state, and if the TP of recrystallization is assumed to be independent of the internal stresses, and if hardening and recovery are neglected (as can be done for static processes), the Markov process reduces to a single differential equation (map)

$$x_{t+\delta t} = x_t + (1 - x_t) R(x_t, T) \delta t \tag{5}$$

where x_t is the degree of crystallization at time step t, $R(x_t,T)$ is the TP of crystallization (which has to be determined as a function of x_t and temperature T) and δt is a time increment. The degree of crystallization in eqn. (5) has been derived from the ratio of flow units in the undistorted state and the total number of flow units.

If the TP of crystallization is chosen, for example, as

$$R(x_t) = A/\delta t x_t$$

eqn. (5) becomes identical with the logistic map, where for sufficiently high values of $A/\delta t$, deterministic chaos occurs. This kind of behaviour has not been observed during crystallization or recrystallization. It does not make physical sense; therefore it is assumed that eqn. (5) can be transformed into a differential equation, without losing physically relevant information, to give

$$\dot{x} = (1 - x) R(x, T) \tag{6}$$

Equation (6) provides a general description of the crystallization process, where only the function of the TP has to be determined. In order to stay in contact as far as possible with the JMAK theory, the TP will be chosen by analogy with the JMAK theory, so that in the isothermal case eqns. (6) and (3) give the same results.

In the JMAK theory it is assumed that grain or crystal nuclei are distributed statistically and that grains or crystals are growing independently from each other. Impingement of grains or crystals is possible, leading to an

extended volume and extended degree of (re-)crystallization, x_{ext}, that has to be transformed into the real degree of (re-)crystallization using

$$dx = (1 - x)\, dx_{ext} \tag{7}$$

A comparison of eqn. (7) with eqn. (6) of the Markov model shows that

$$\dot{x}_{ext} \equiv R_{JMAK}(x,T) \tag{8}$$

Integration of eqn. (7) and comparison of the result with eqn. (3) yields

$$x_{ext} = \alpha t^n \tag{9}$$

The time derivative of eqn. (9) is as follows:

$$\dot{x}_{ext} = K_1(-\ln|1-x|)^{K_2} + \dot{T}\frac{-\ln|1-x|}{1-K_2}\left(\frac{K_1'}{K_1} - \frac{K_2'}{1-K_2} + K_2' \ln|-\ln|1-x||\right) \tag{10a}$$

where

$$K_1 = \alpha^{1/n} n \text{ and } K_2 = (n-1)/n \tag{10b}$$

$$K_1' = dK_1/dT \text{ and } K_2' = dK_2/dT \tag{10c}$$

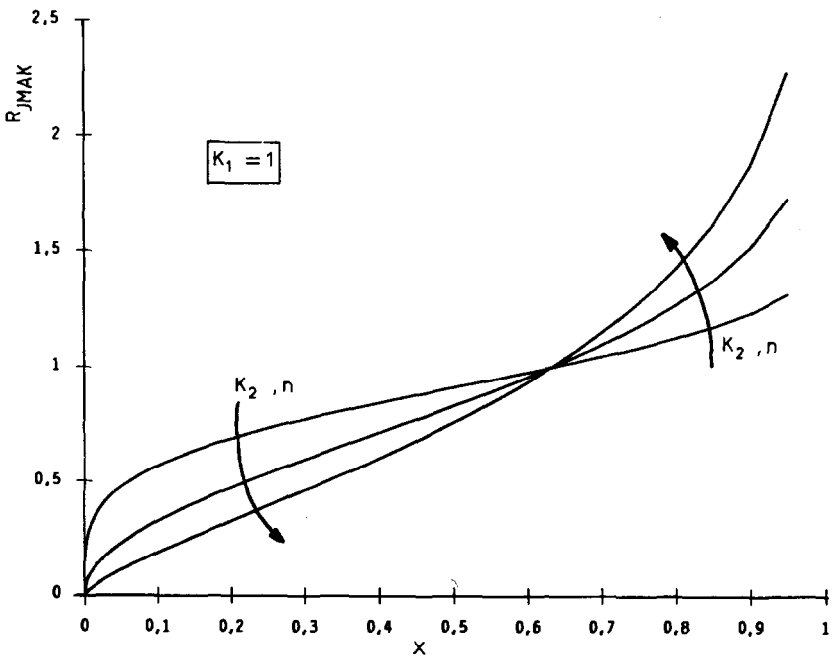

Fig. 2. Influence of the Avrami parameter n or K_2 on the TP derived from the JMAK theory (eqn. (10a) for $\dot{T} = 0$).

For isothermal processes, the temperature derivatives are equal to zero, so that only the first part of eqn. (10a) has to be used. In fact, the second part of eqn. (10a) is irrelevant for the TP of crystallization. This will be shown in the non-isothermal calculations.

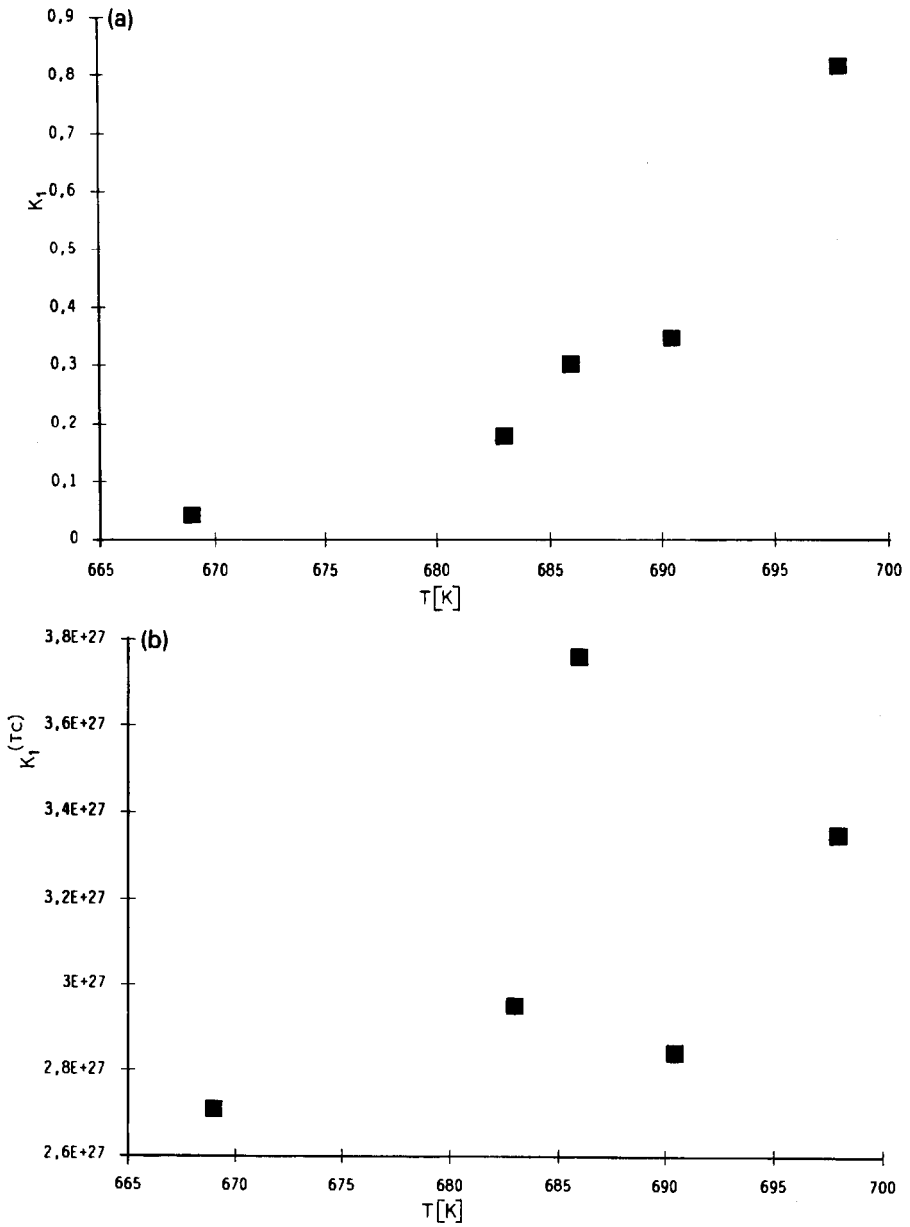

Fig. 3. Temperature dependence of the Avrami parameter (a) K_1, and (b) its temperature compensated form, $K_1^{(TC)}$.

DETERMINATION OF PROCESS PARAMETERS

Avrami parameters

The Avrami parameters, α and n in eqn. (3) or K_1 and K_2 in eqn. (10), are determined from isothermal experiments, not by an Avrami plot but by a different strategy. As according to experience the JMAK theory describes the first two-thirds of the transformation process sufficiently well, emphasis is put on fitting $R(x,T)$, especially to this region of x.

Figure 2 demonstrates the influence of K_2 on the TP of crystallization (eqn. (10a) for $\dot{T} = 0$). Equation (10a) shows that for $-\ln|1-x| = 1$, i.e. $x = 0.63212$, K_2 has no influence on the TP of crystallization. Thus, K_1 is determined easily at $x = 0.63$ from eqn. (6). Figure 3 shows the temperature dependence of K_1 and its temperature-compensated form

$$K_1^{(TC)} = K_1 \exp(Q/RT)$$

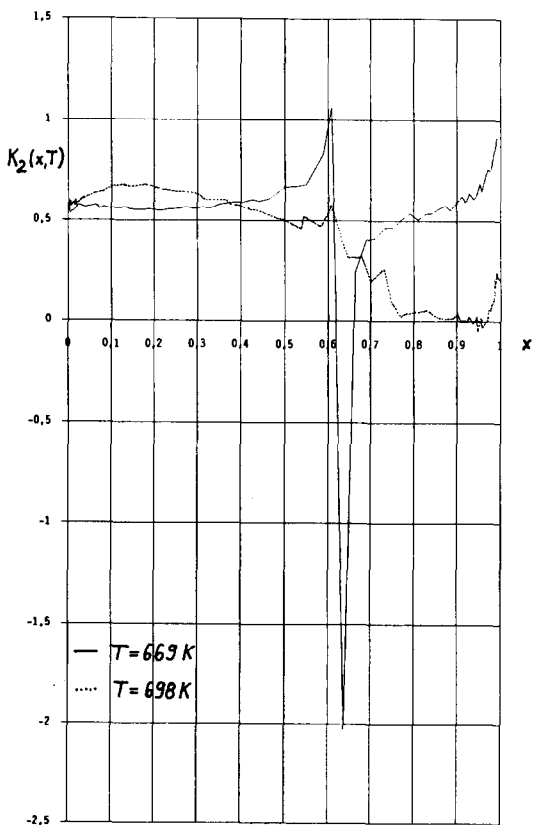

Fig. 4. Temperature dependence of K_2 according to experiment (cf. eqn. (11)) for two temperatures.

where Q is the activation energy of the whole crystallization process as determined experimentally, R is the gas constant and $Q/R = 44\,379.232$ K. There is a small linear dependence of $K_1^{(TC)}$ on the temperature, leading to the empirical relationship

$$K_1^{(TC)} = K_{11} + K_{12}T$$

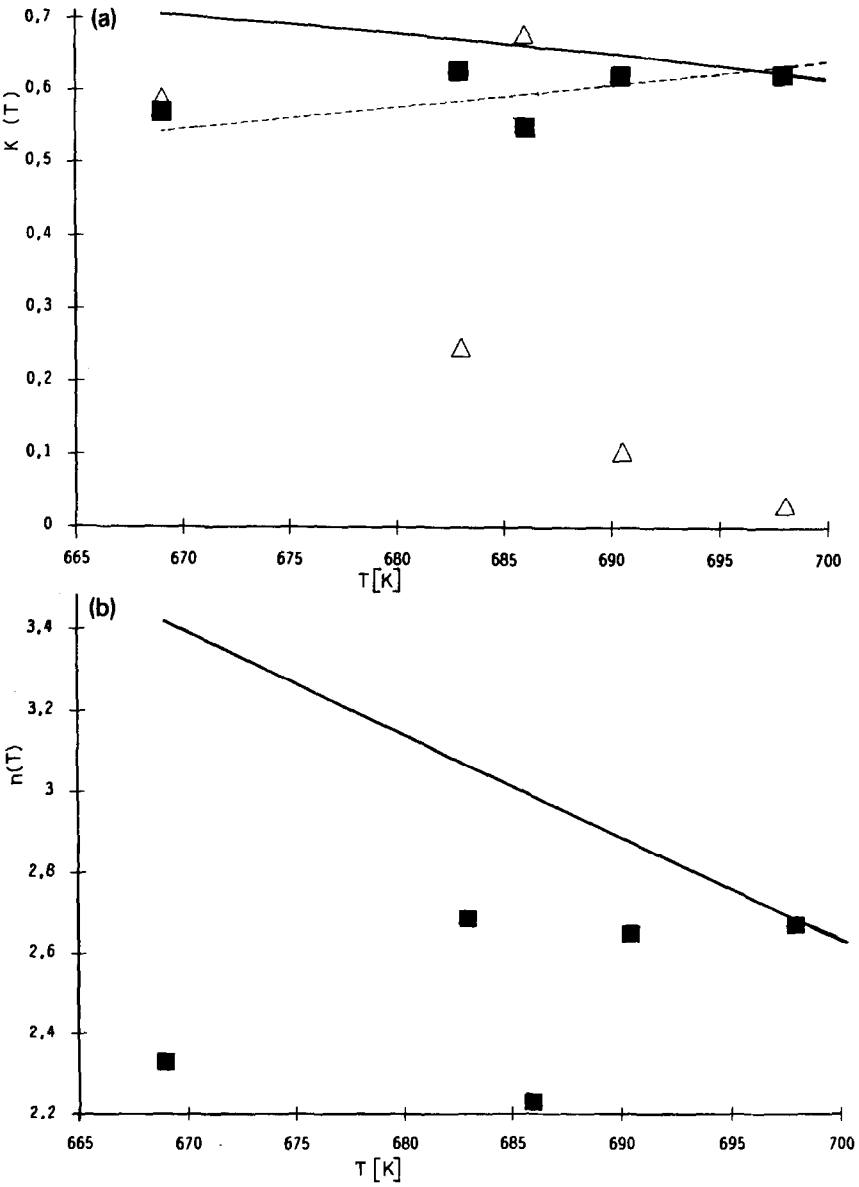

Fig. 5. Temperature dependence of (a) K_2, and (b) n at different degrees of crystallization: ■, $x = 0.05$; △, $x = 0.9$: ——, K_2 and n according to the classical Avrami method leading to mean values for K_2 and n; - - - - - -, K_2 fitted to the data points of $x = 0.05$.

with $K_{11} = -1.036\,046\,905\,657\,23 \times 10^{28}$ and $K_{12} = 1.967\,796\,100\,477\,53 \times 10^{25}$ K^{-1}, when fitted to the data by a least-squares procedure. With K_1 given, an estimate of K_2 can be calculated by solving eqn. (10a) for K_2:

$$K_2 = \frac{\ln|\dot{x}/K_1(1-x)|}{\ln|-\ln|1-x||} \tag{11}$$

In Fig. 4, the results of eqn. (11) are drawn for two temperatures. The mathematical discontinuity at $x \approx 0.63$ is only partly reflected by the data because the data points have not been recorded densely enough. Figure 5(a) shows the temperature dependence of K_2 for different values of x: for small x, K_2 increases with temperature, whereas for large x it decreases. Increasing K_2 below $x = 0.63$ means a decreasing TP, decreasing K_2 above $x = 0.63$ results in a decreasing TP as well, so that, as far as K_2 or n is concerned, the TP would decrease with increasing temperature. In any case, K_2 is a linear function of temperature.

Proceeding in the classical way by fitting the data in an Avrami plot to a linear curve between $x = 0.1$ and 0.95 leads to a mean value of n, which is also shown in Fig. 5.

In order to fit K_2 to the data, $K_2(T)$ at $x = 0.05$ was taken as a first estimate, fitted more closely but only qualitatively at the lowest and highest temperatures of the experiments ($T = 669$ K and 698 K). The temperature dependence inbetween was interpolated linearly, leading to

$$K_2 = K_{21} + K_{22}T \tag{12}$$

with $K_{21} = -1.612\,21$ and $K_{22} = 3.222\,44 \times 10^{-3}$ K^{-1}.

When using data at low values of x, it had to be checked whether the initial disturbance had already decayed. It can be seen from the output of the calorimeter that this is the case already at $x = 0.01$, so that it is fully justified to fit parameters to the lower range of x. Figures 6(a) and 6(c) show the TP, R_{JMAK} over x, for two different temperatures, where the TP has been calculated from experimental data according to eqn. (6). Inserting $\alpha(T)$ and $n(T)$, determined from $K_1(T)$ and $K_2(T)$ by eqn. (10a), into eqn. (3) leads to the results shown in Fig. 7. The value of n obtained from the classical method gives a good average description of the process, but it can be clearly seen that the shape of the $\dot{x}$–t curve deviates from the experimental one: the process accelerates too slowly. The $\dot{x}$–t curve with the K_2 from eqn. (12) has the right shape, but the real process does not begin until after a time delay. This proves the findings of Göbel [4] that obtaining a good fit of the data for a plot of TP vs. x leads to a good description of the whole process (cf. Fig. 7(c)), but this also means that the delay time has to be included in the model as an additional variable.

Incubation time

The delay or incubation time t^* is the time at which the calorimeter gives the first stable signal. Physically, this means that the crystallization reaction

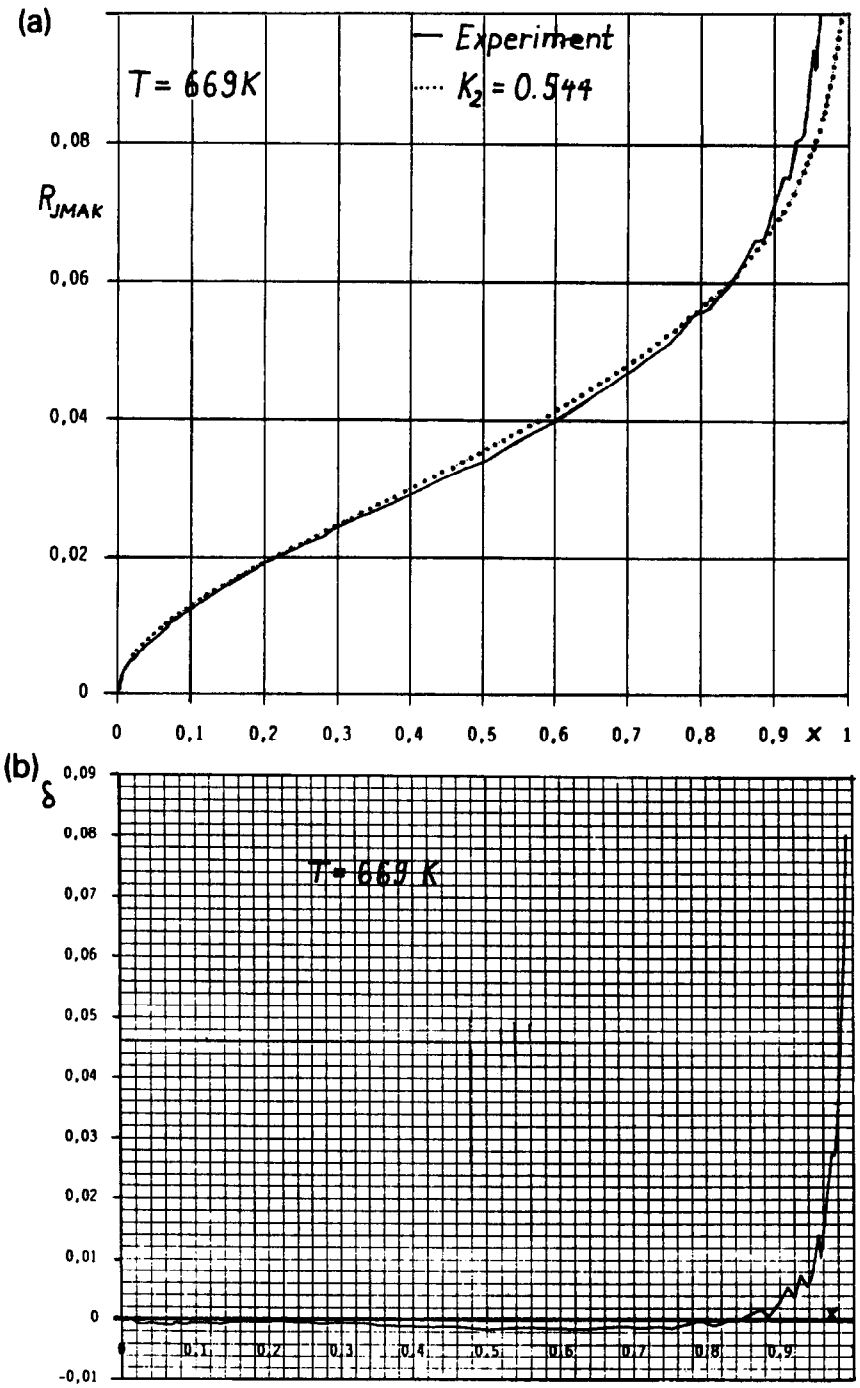

Fig. 6. The TP according to the JMAK theory and the deviations of the experimental data therefrom at two temperatures: (a) experimental and theoretical TP at $T = 669$ K; (b) difference between measured and calculated TP; (c) as in (a), for $T = 698$ K; (d) as in (b), for $T = 698$ K.

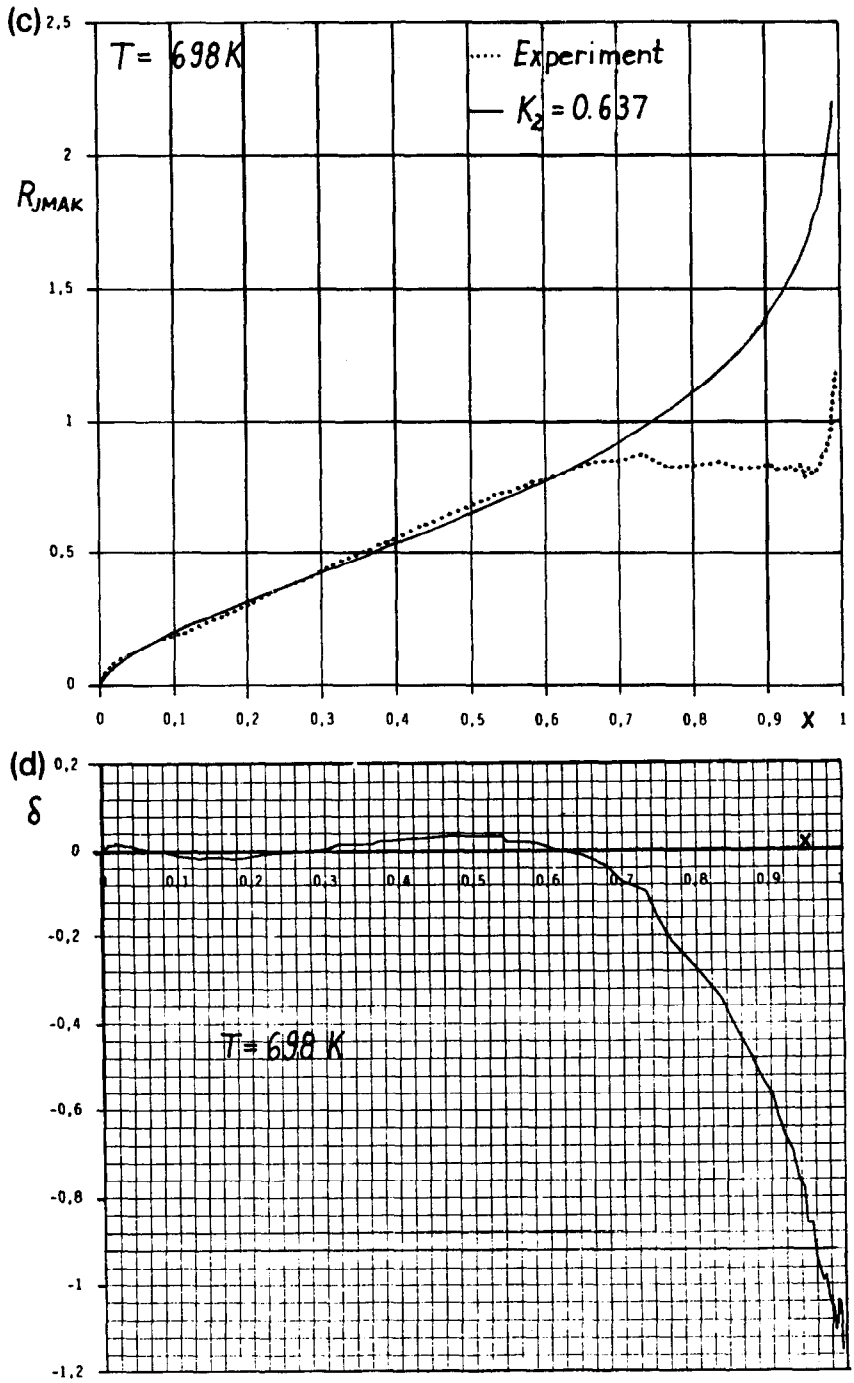

Fig. 6 (continued).

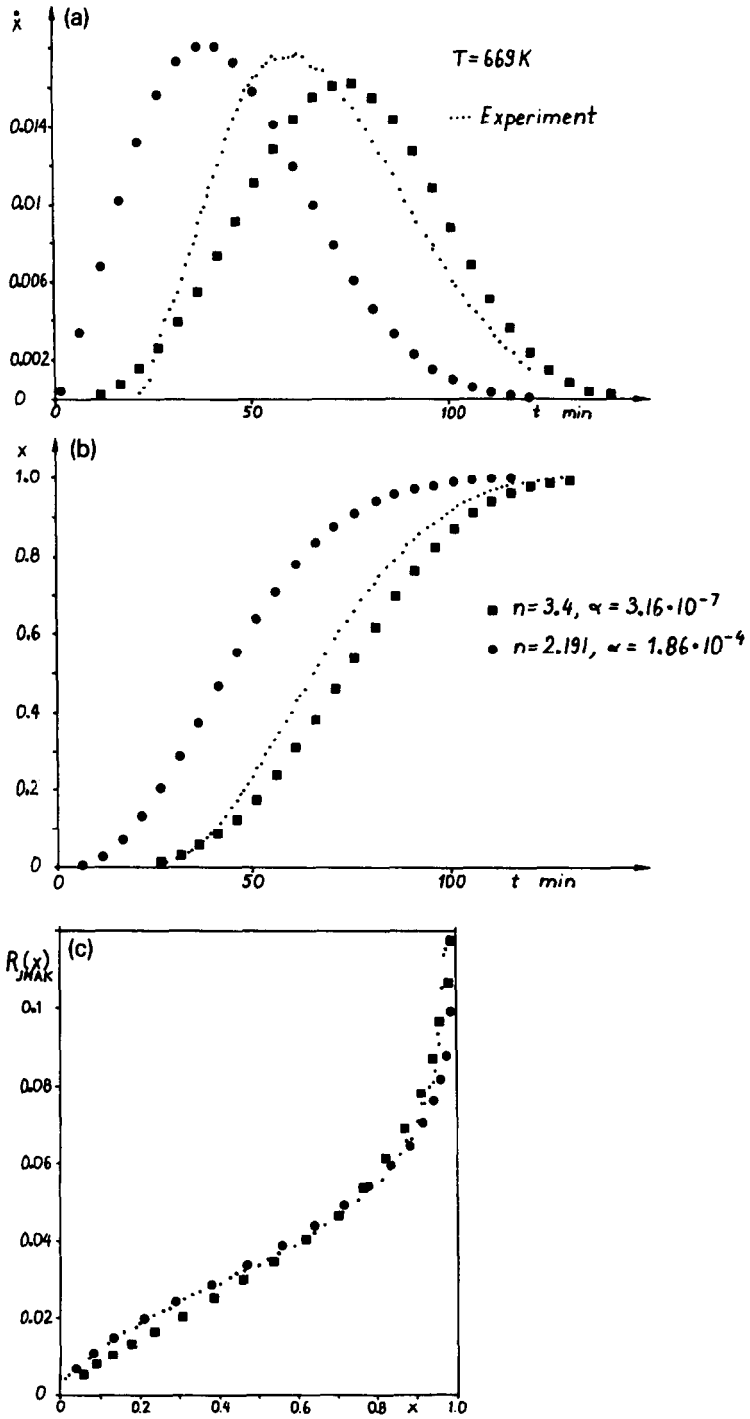

Fig. 7. Comparison between the temperature-dependent Avrami parameters: ·····, experimental data; ■, results for the classical method of determining the Avrami parameters; ●, results for the method developed here. The Avrami equation (eqn. (3)) has been used to calculate the following at $T = 669$ K: (a) rate of x vs. time; (b) x vs. time; (c) TP according to JMAK vs. x.

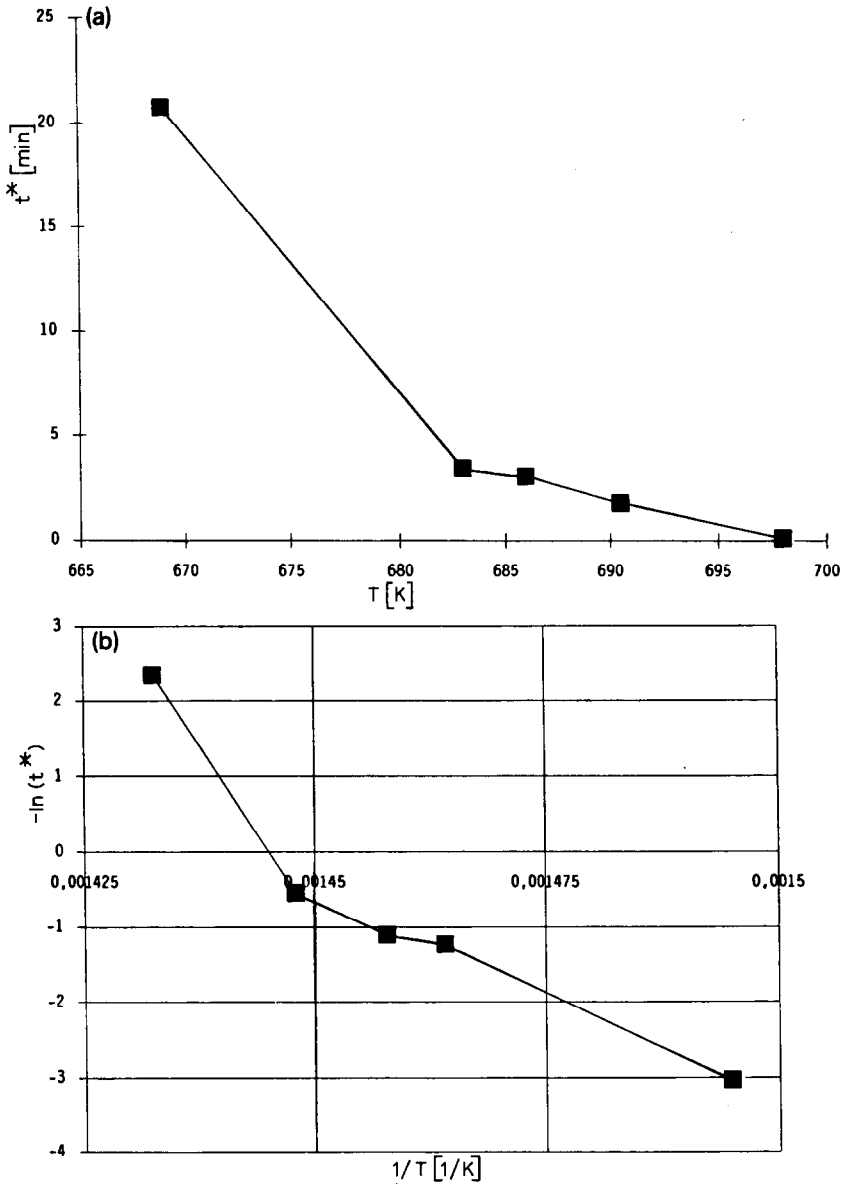

Fig. 8. Temperature dependence of the incubation time: (a) linear plot; (b) logarithmic plot vs. T^{-1}, where the slope of a linear curve gives the activation energy of an Arrhenius model.

has just begun. Figure 8(a) shows that the incubation time decreases with increasing temperature, and that it has a non-linear dependence on temperature. It is assumed that the incubation time is determined by a thermally activated process. Thus, a plot of $\ln|t^*|$ vs. $1/T$ should give a linear function of the data. Figure 8(b) shows that the data points either lie very

much scattered, or that the process is not simple. Fitting the data points of Fig. 8(b) to the empirical function

$$\frac{1}{t^*} = \frac{1}{t_0^*} \exp\left(-\frac{Q^*}{R}\frac{1}{T}\right) \tag{13}$$

leads to $Q^*/R = 78\,545.4539$ K, which is almost twice the activation energy of the whole crystallization process. Omitting the data point at $T = 698$ K gives an activation energy that is of the same order of magnitude as Q/R, with $Q^*/R = 52\,830.955$ K.

Consequently, it might be more appropriate to determine a temperature dependent activation energy, where Q^* increases with the temperature (cf. Fig. 9(a)). A similar relationship has been derived for the activation energies of creep by Tegart and Sherby [7]. They explain the rise in activation energy by the contributions of two parallel processes (see Fig. 9(b)), leading to

$$Q = \frac{w_1 Q_1 \exp(-Q_1/RT) + w_2 Q_2 \exp(-Q_2/RT)}{w_1 \exp(-Q_1/RT) + w_2 \exp(-Q_2/RT)} \tag{14a}$$

where the activation energies of the partial processes follow from their strain rates

$$\dot{\epsilon}_1 = w_1 \exp(-Q_1/RT) \text{ and } \dot{\epsilon}_2 = w_2 \exp(-Q_2/RT) \tag{14b}$$

The total strain rate is the sum of the partial strain rates. Here, the strain rate has to be replaced by the inverse of the incubation time, according to eqn. (13). For $T \to \infty$, it follows from eqn. (14a) that

$$Q^*|_{T\to\infty} = Q^*_{\max} = \frac{w_1 Q_1 + w_2 Q_2}{w_1 + w_2} \tag{14c}$$

while at low temperatures only one process makes a contribution, for example leading to

$$Q^*_{\min} = Q_2 \equiv Q^* \tag{14d}$$

Hence it follows from eqn. (14c) for $Q^*_{\max} = m\ Q^*_{\min}$ that

$$Q_1 = Q^*[m + (m-1)w_2/w_1] \tag{14e}$$

The ratio w_1/w_2 is estimated by estimating the transient values of temperature and activation energy, T_t and Q_t^*, inserting both into eqn. (14a) and solving it for w_2/w_1. With

$$Q_t^* = A^* Q^*$$

it follows for $w_2/w_1 > 0$

$$\frac{w_2}{w_1} \approx \frac{m - A^*}{A^* - 1} \exp\left[-\frac{Q^*}{RT_t}(m-1)\right] \tag{14f}$$

Submitting the experimental data to this procedure leads to the following set

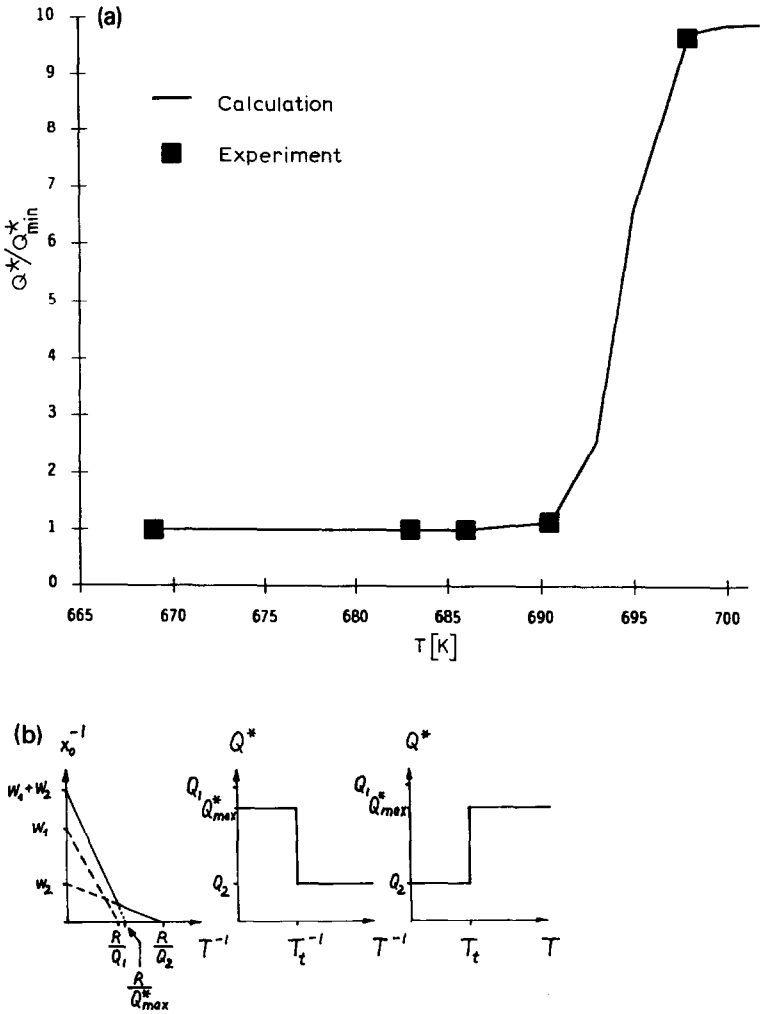

Fig. 9. Temperature dependence of the activation energy for the incubation time: (a) Comparison between the experimental and the calculated values. The experimental data of Q^* were obtained from Fig. 10(b): Q^*_{min} was estimated from the slope between the second and last data point. Q^*_{max} is the slope between the two first data points. The theoretical curve was obtained with $Q^*_{min} = 56148.936$ K, $A^* = 6.6$, $T_t = 695$ K, $m = 9.9106$. (b) Additional contributions of two processes to the activation energy, shown schematically for linear functions, leading to an increase in the activation energy with increasing temperature.

of parameters: $Q^*_{min}/R = 56148.94$ K; $m = 9.91$; $A^* = 6.60$; $T_t = 695.00$ K. Figure 9(a) shows that the experimental results are described very well.

After the temperature dependence of the incubation time has been determined, the latter has to be related to the TP of crystallization. The delay time is considered by an additional TP

$$R_{inc} = 1 - \exp(-x/x_0) \tag{15}$$

that varies between zero, at $x = 0$, and unity, when x is large; x_0 is a function of the incubation time.

It is assumed that the crystallization process is impeded at small values of x by a second process related to, for example, the stabilization of crystal nuclei. This leads to a multiplication of the TPs from eqns. (10a) and (15):

$$R(x,T) = R_{\mathrm{JMAK}}(x,T) \cdot R_{\mathrm{inc}}(x,T) \tag{16}$$

The product of two probabilities expresses the probability of an event that takes place when two separate events are realized. When tossing a coin, for example, the probability of tossing heads after tails is equal to the product of the probabilities of tossing heads and tails, respectively.

The TP of eqn. (16) is equal to zero for $x = 0$. Thus, with eqn. (6), the crystallization process could not start at all. The random fluctuations that cause the process to start in reality also have to be introduced. This is done by a small constant, R_0 or $R_0 \exp(-x/x_0)$, which is added to eqn. (16). It is calculated as $R_0 = 1 \times 10^{-8}$ min^{-1}, because for this value there are no considerable differences between the results from eqns. (3) and (6) and the JMAK TP of eqn. (10a). Calculating with a decreasing TP of fluctuations, $R_0 \exp(-x/x_0)$, assumes that the number of sites favourable for the creation of crystal nuclei decreases with increasing x. The differences between the two TPs for fluctuations are small.

The entire differential equation for the crystallization thus runs as follows:

$$\dot{x} = (1-x)\left\{K_1[-\ln|1-x|]^{K_2}[1-\exp(-x/x_0)] + R_0 \exp(-x/x_0)\right\} \tag{17}$$

Equation (17) was integrated while x_0 was changed until the result was near the experimental incubation time. Figure 10(a) shows that x_0 and t^* are proportional to each other: $x_0 = \Phi t^*$ with $\Phi = 3.373 \times 10^{-6}$ min^{-1}. In Fig. 10(b), x_0 is drawn in a logarithmic plot to show its dependence on $1/T$ and thus its activation energy.

When the incubation time is included in the Avrami plot, drawing $\log(-\ln|1-x|)$ vs. $\log(t-t^*)$, the data form a sequence of linear sections (cf. Fig. 1(b)). Determining n from the time-transformed Avrami plot for small values of x gives about the same results as determining n from the plot of the TP vs. x.

Correcting the TP of JMAK

In Figs. 6(b) and 6(d), the difference δ between measured and JMAK TP is drawn:

$$\delta = \frac{\dot{x}}{1-x} - R_{\mathrm{JMAK}} \tag{18}$$

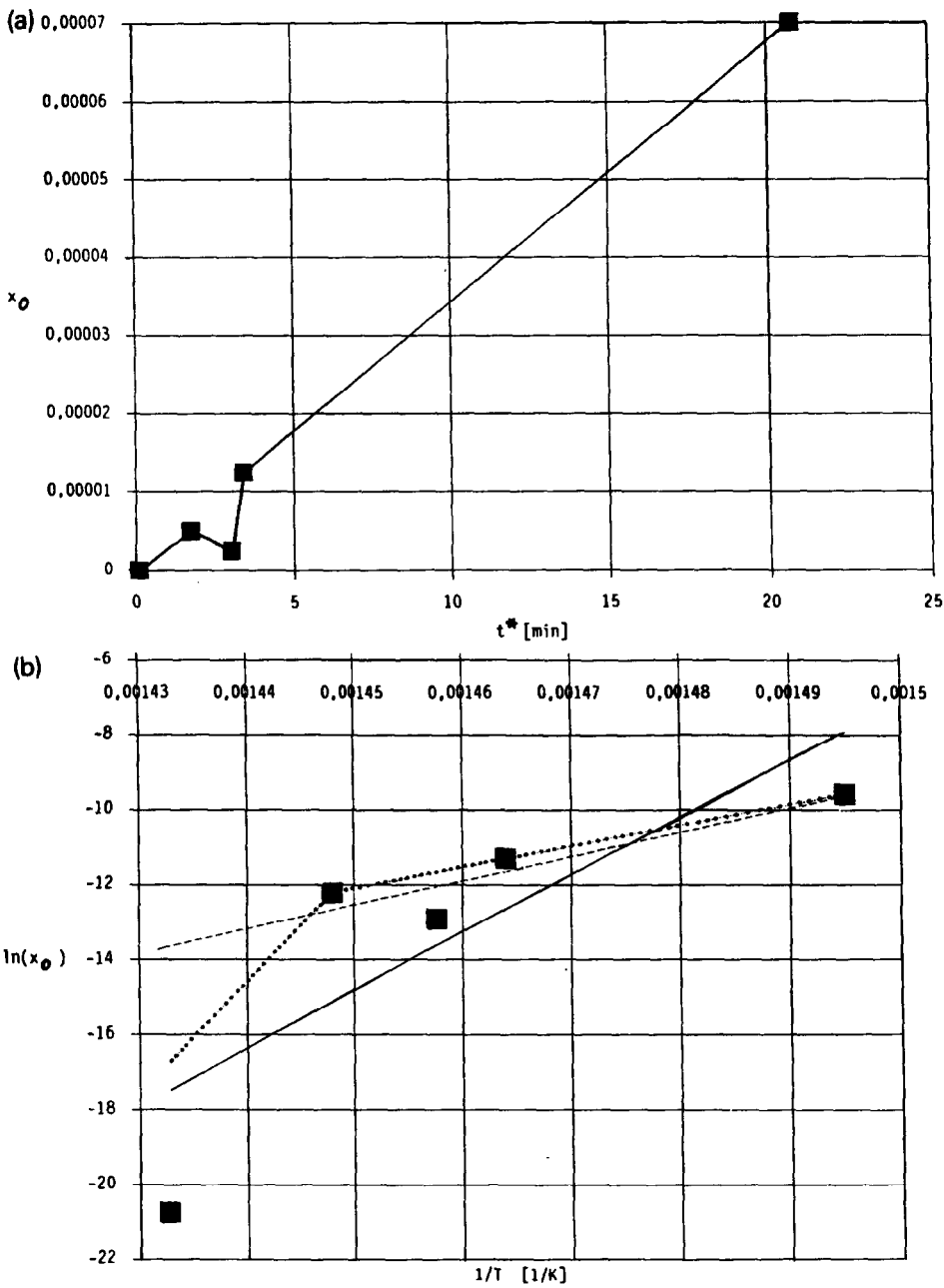

Fig. 10. Determination of the incubation variable x_0 in the TP of crystallization: (a) dependence on the incubation time; (b) temperature dependence. Black squares give values of x_0 determined by integration of eqn. (17). In (b), the slope of the solid line is $Q^*/R =$ 153272.209 K, for the broken line it is $Q^*/R = 64598.986$ K. The dotted curve shows $Q^*(T)$ determined as in Fig. 8(b); reduction of T_f leads to a better fit of $Q^*(T)$ to the data.

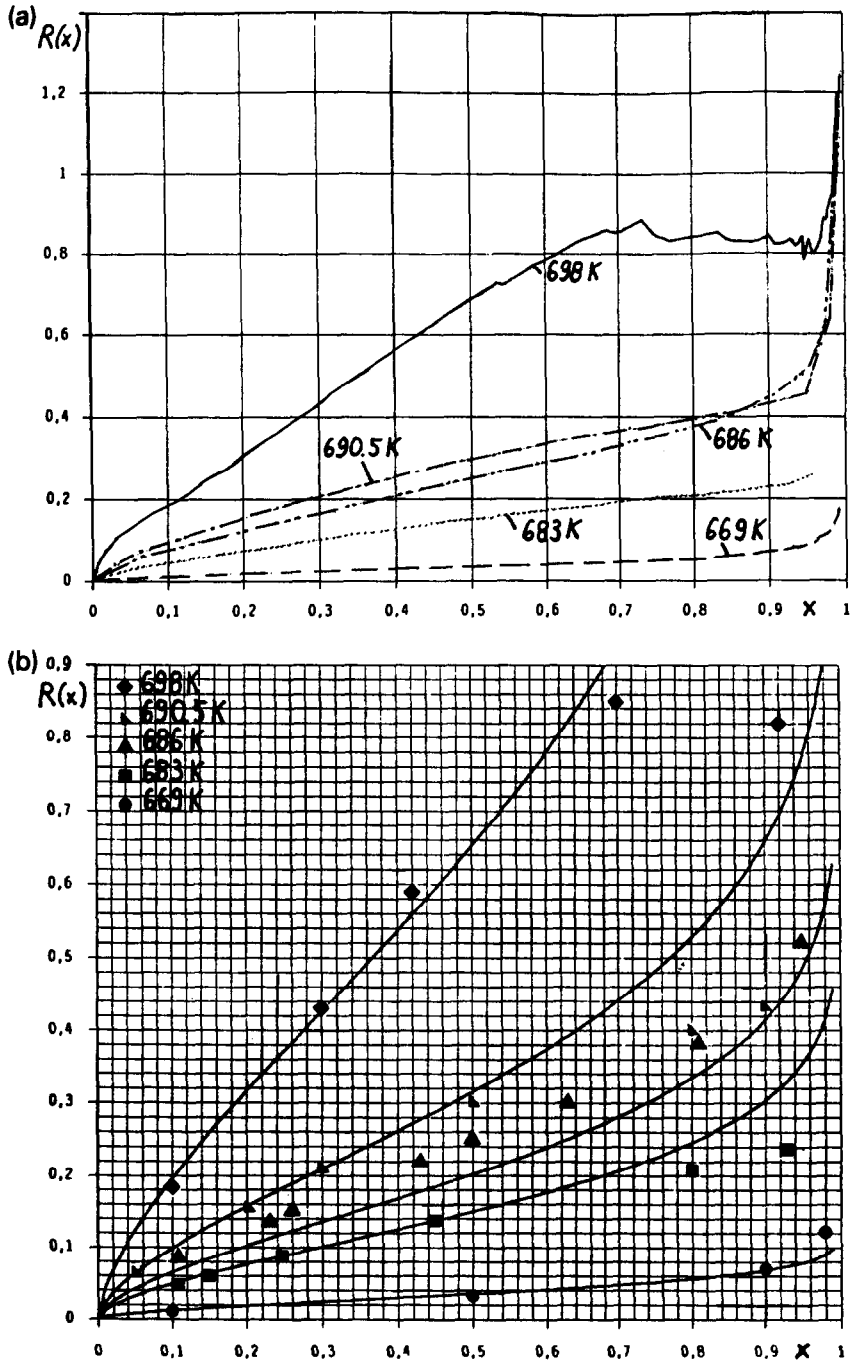

Fig. 11. Comparison between experimental and theoretical TPs of crystallization: (a) experimental data, $\dot{x}/(1-x)$; (b) TPs according to the JMAK theory (eqn. (10a)) shown with some experimental data points; (c) the same as in (b) but with a corrected JMAK TP, $R(x) = R_{\mathrm{JMAK}} + \delta$.

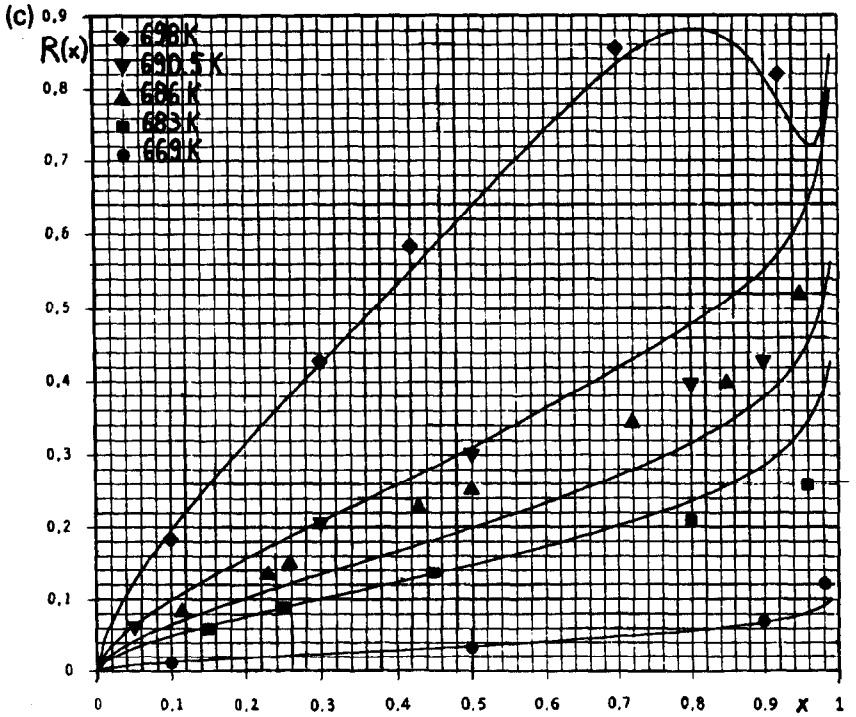

Fig. 11 (continued).

This shows that in the last third of the process, deviations between experimental and JMAK behaviour occur. At the lowest temperature, $T = 669$ K, the process accelerates when compared with the theory, whereas at the highest temperature the process is considerably slower than predicted. The correcting TP, eqn. (18), is determined using an empirical function

$$\delta(T) = A(T)\{\exp[B(T)x] - 1\} \tag{19}$$

where A and B are temperature-dependent parameters that have to be fitted to the experimental data. Equation (19) gives $\delta = 0$ at $x = 0$, so that it does not contribute to initial fluctuations. Parameters A and B were roughly estimated for $T = 669$ K and 698 K by the approximate function

$$\delta = A \exp(Bx) \tag{19a}$$

where the error between eqns. (19) and (19a) is small for small A and large B. Then the temperature dependence of A and B was interpolated by the linear functions

$$A = A_1 + A_2 T$$

with $A_1 = 3.447 \times 10^{-3}$ and $A_2 = -5.153 \times 10^{-6}$ K^{-1}, and

$$B = B_1 + B_2 T$$

with $B_1 = -137.053$ and $B_2 = 0.2095$ K^{-1}.

In Fig. 11, the results for different TPs can be compared. Figure 11(b) shows the JMAK TP of eqn. (10a) with $\dot{T} = 0$. In Fig. 11(c), the corrected TP

$$R = R_{JMAK} + \delta \tag{20}$$

is drawn, together with some of the experimental data points. It can be seen that A and/or B are probably not linear functions of the temperature, but as a matter of fact the last curve ($T = 698$ K) is described very well by the corrected TP.

The physical reasons for deviations from JMAK behaviour can only be guessed. The stochastic rules admit three possibilities for the additional component in the TP of crystallization (eqn. (20)). An event means a contribution to crystallization by whatever process.

(a) The two events are stochastically disjunct: the two processes are alternatives happening independently of each other so that $\delta \equiv R_{\text{corr}}$.

(b) The two events are stochastically independent: The two processes do not influence each other, but they overlap in the event space so that $\delta = R_{\text{corr}} - R_{\text{JMAK}} \times R_{\text{corr}}$.

(c) The two events are neither stochastically disjunct nor independent: this is the least-restricted case with $\delta = R_{\text{corr}} - R(E_{\text{JMAK}} \cap E_{\text{corr}})$, where E stands for event.

For cases (a) and (b), knowing R_{JMAK} and δ leads to the determination of R_{corr}, which may help in discussing the kinetics of the crystallization process.

NON-ISOTHERMAL PROCESSES

Isothermal processes are very convenient for theoretical considerations but they are difficult to perform experimentally. Thus, non-isothermal processes performed at constant heating rate are of growing interest for experiments. For the Markov model, after having determined the temperature dependence of all parameters, only a differential equation for the temperature has to be introduced in addition to eqn. (17):

$$\dot{x} = (1 - x)\{[R_{\text{JMAK}} + \delta] R_{\text{inc}} + R_0 \exp(-x/x_0)\} \tag{21a}$$

$$\dot{T} = H \tag{21b}$$

where H is the heating rate. The TPs and x_0 are functions of temperature. In the cases of linear temperature dependence, negative values of K_1, K_2 and B are avoided by cutting off the negative parts, replacing them by zero. Thus, at low temperatures the TPs of crystallization are zero (which is physically convincing). For the JMAK-correcting TP, a maximum value for B had to be fixed. Once this value has been reached at $T = 698$ K it stays constant because, otherwise, negative TPs would occur. Another problem

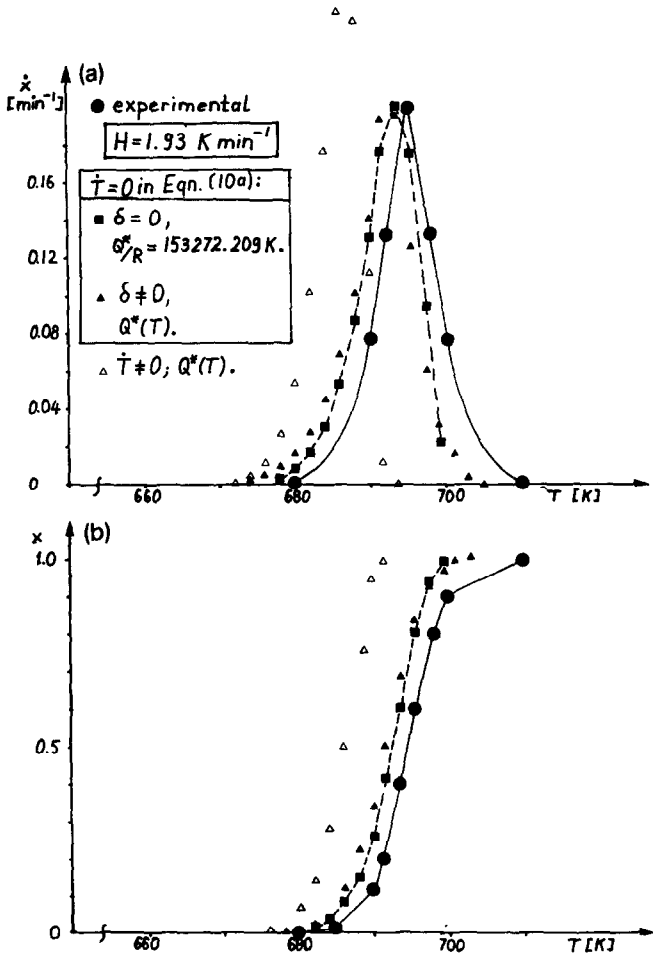

Fig. 12. Comparison between theory and experiment for non-isothermal crystallization.

was the calculation of $Q^*(T)$ at low temperatures, where Q^* and x_0 approach infinity, so that numerical values that leave the numerical range of the computer must be avoided.

Calculations for non-isothermal processes have been performed for different TPs and parameters. There are two important cases: (a) JMAK TP without temperature gradient (eqn. (10a)); (b) no JMAK correction ($\delta = 0$).

The TP for the delay time R_{inc} as well as the TP for random fluctuations are always included. Figure 12 compares an experiment with calculations for different assumptions on the TPs. The best results are achieved with omission of both, the temperature gradient as well as the JMAK correction in the TP for crystallization. Moreover, the consideration of a temperature-dependent activation energy for the incubation time did not improve the results appreciably. It is fully sufficient to operate with a constant activation energy Q^*. Hence, the best results are achieved with the simplest of models.

Having a JMAK TP without a temperature gradient, although this gradient would be mathematically correct, means that the physical system reacts only to the actual temperature. It does not sense a temperature gradient. Although the heating rate is not particularly slow, the system acts as if it is in a quasi-static process. A very convincing explanation of this behaviour is [8] that Markov processes have no memory but react to a given state only. Thus, these systems cannot detect time gradients because they would have to know what was happening in the last time step, or they would have to anticipate what is going to occur in the next one. It can thus be concluded that a Markov process is an appropriate means of describing crystallization.

CONCLUSIONS

The intention of this paper is to provide help in handbook style for analysing calorimetric data on (re-)crystallization. It has been shown for the Co–Zr alloy investigated here that the value of the Avrami parameter n depends on the method of determination. The methods developed here for the determination of the Avrami parameters α and n have the advantage of describing the experimental data far better than is done by parameters determined by the classical method. As in the material investigated here, the crystallization process is preceded by a temperature-dependent incubation time, a third process variable had to be determined additionally. A minimum of seven constants (Q, K_{11}, K_{12}, K_{21}, K_{22}, Q^* and Φt_0^*) is then sufficient to calculate isothermal as well as non-isothermal processes with tolerable accuracy.

The calculations of the non-isothermal process show that the crystallizing material has Markov properties, i.e. it does not react to temperature gradients but only to actual temperatures. Thus, it becomes theoretically clear how to connect isothermal with non-isothermal crystallization.

Besides a quantitative description of the crystallization process, the second objective behind our analysis of calorimetric data is the discussion of the reaction kinetics. This will be done in a forthcoming paper.

ACKNOWLEDGEMENTS

Funding from the Deutsche Forschungsgemeinschaft, Sonderforschungsbereich 319, is gratefully acknowledged. We appreciate the helpful advice given by Professor Dr. F. Haessner.

REFERENCES

1 W.A. Johnson and R.F. Mehl, Trans. Am. Inst. Min. Met. Eng., 135 (1939) 416.
M. Avrami, J. Chem. Phys., 7 (1939) 1103; 8 (1940) 212; 9 (1941) 177.
A.E. Kolmogorov, Izv. Akad. Nauk SSSR, Ser. Mat., 1 (1937) 355.

2 J. Schmidt, Doctoral Thesis, Braunschweig, 1990.
3 K.H. Schönborn and F. Haessner, Thermochim. Acta, 86 (1983) 305.
4 I.R. Göbel, Int. J. Plast., 7 (1991) 161.
5 M.M. Nicolaus, Thermochim. Acta, 151 (1989) 345.
6 E.A. Steck, Int. J. Plast., 1 (1985) 243.
7 W.J.M. Tegart and O.D. Sherby, Philos. Mag., 3 (1958) 1287.
8 E.A. Steck, personal communication, 1990.